Biol Trace Elem Res (2015) 168:508–515
DOI 10.1007/s12011-015-0369-5

Spectroscopic Evaluation of DNA–Borate Interactions

Ayse Ozdemir[1,2] · **Omer Faruk Sarioglu**[1,2] · **Turgay Tekinay**[3,4]

Received: 2 March 2015 / Accepted: 12 May 2015 / Published online: 21 May 2015

Abstract We describe the binding characteristics of two natural borates (colemanite and ulexite) to calf thymus DNA by UV–vis absorbance spectroscopy, circular dichroism (CD) spectroscopy, Fourier transform infrared (FT-IR) spectroscopy, and a competitive DNA binding assay. Our results suggest that colemanite and ulexite interact with calf thymus DNA under a non-intercalative mode of binding and do not alter the secondary structure of the DNA helix. The FT-IR spectroscopy results indicate that the two borates might interact with DNA through sugar-phosphate backbone binding.

Keywords Calf thymus DNA · DNA binding · Spectroscopy · Boron · Deoxyribose sugar

Abbreviations

CD	Circular dichroism
Col	Colemanite
CT-DNA	Calf thymus DNA
FT-IR	Fourier transform infrared
Ule	Ulexite
UV–vis	Ultraviolet–visible

✉ Turgay Tekinay
ttekinay@gazi.edu.tr

[1] Institute of Materials Science & Nanotechnology, Bilkent University, 06800, Bilkent, Ankara, Turkey

[2] UNAM-National Nanotechnology Research Center, Bilkent University, Ankara 06800, Turkey

[3] Department of Medical Biology and Genetics, Faculty of Medicine, Gazi University, 06500, Besevler, Ankara, Turkey

[4] Life Sciences Application and Research Center, Gazi University, 06830, Golbasi, Ankara, Turkey

Introduction

Boron is a trace element commonly found in sedimentary rocks, shales, oceans, and the soil. It typically exists as boric acid, borosilicate, borax, or borate minerals such as ulexite (ule), colemanite (col), or kernite [1]. Borates are widely used in industrial processes for the production of glass, cement, flame retardants, and cellulosic and isolation materials; other anthropogenic sources of boron include borate mining, wood burning, sewage disposal, and weathering processes [1]. Borates are also used as pesticidal, herbicidal, and fungicidal agents, which present a major route of human exposure to boron compounds [2]. Nevertheless, borates and other boron compounds are generally considered non-toxic. In addition, boron contributes to nucleic acid, lignin, and carbohydrate biosynthesis; plays an important role in maintaining membrane integrity and seed production mechanisms in plants [2, 3]; and is suggested to be vital for membrane signaling, reactive oxygen species removal, and the metabolism of certain hormones (e.g., insulin, estrogen and testosterone) in animals [4, 5]. However, the amount required for these functions is minimal, and the role of boron in the animal metabolism is not properly understood. Boron compounds have also been reported as inhibitors of DNA damage [6] induced by titanium dioxide and paclitaxel, but the mechanism involved is unknown [7–9]. In contrast, there are some reports in the literature about the dose-dependent anticancer activity and growth inhibition properties of boric acid, which suggests that, although an essential element in low concentrations, boron compounds can target various biomacromolecules to inhibit cell growth and induce apoptosis at higher doses [10]. As such, spectroscopic evaluation of the interaction between borates and DNA may provide useful information regarding the effect of these compounds on the DNA structure at different concentrations and shed light on the mechanism by which borates prevent DNA damage.

The present study details the DNA binding characteristics of the natural borates ulexite (ule) and colemanite (col) under

physiological conditions. Alterations in the secondary structure of DNA are evaluated, and the binding modes responsible for these changes are investigated utilizing various spectroscopic analysis techniques. The borates were chosen for their widespread use in industrial applications [11].

Materials and Methods

Materials and Solutions

Ultrapure Calf thymus DNA (CT-DNA) (CAT No. 15633–019) was purchased from Invitrogen, CA and used as supplied. pUC19 plasmid DNA and Quick-Load® 1 kb DNA ladder were purchased from New England Biolabs, UK. Tris(hydroxymethyl)aminomethane (Tris) and ethidium bromide (EtBr) were purchased from Sigma-Aldrich Chemicals, USA. $Ca_2B_6O_{11}{\cdot}5H_2O$ (CAS No. 1318-33-8, ~92 % pure) and $NaCaB_5O_9{\cdot}8H_2O$ (CAS No. 1319-33-1, ~93 % pure) were supplied from Eti Mine Works General Management, Turkey. The chemical structures of two borates were drawn with ACD/ChemSketch (Advanced Chemistry Development Inc., Canada) software (Fig. 1) based on the structures that are presented previously [12, 13]. All reagents were used as supplied without further purification. Ten millimolars Tris–HCl buffer (pH 7.4) was used as buffer medium in all experiments. Buffer pH was adjusted using HCl.

Stock solutions of borates were prepared by dissolving boron compounds to a concentration of 1.0 M in double-distilled water. Stock solutions were diluted as necessary to obtain the desired concentrations prior to each experiment. Ultrapure water was used for the preparation of all solutions.

DNA stock solutions (0.1 mg/ml DNA, or 1.18×10^{-4} M base pairs) [10] were obtained by dissolving CT-DNA in 10 mM Tris–HCl buffer. Molarities of CT-DNA solutions were confirmed by spectrophotometric analysis, assuming ε_{260}=6600 M^{-1} cm^{-1} [11]. The ratio of absorbances at 260 and 280 nm was checked to verify solution purity and found to be 1.8, indicating that the DNA solution was satisfactorily free of protein [14].

UV–Visible Spectroscopy

UV–vis absorbance measurements were performed on a Thermo Scientific NanoDrop 2000 benchtop spectrophotometer (Thermo-Fisher Scientific, USA). Absorption titration experiments were performed by titrating either varying concentrations of CT-DNA (0.1, 0.2 mM) against a constant concentration of borates (0.1 mM) or varying concentrations of borates (0.001–0.1 mM) against a constant concentration of CT-DNA (0.01 mM). All borate solutions were homogenized through vortexing before each use. Spectra were recorded in the wavelength range of 200–800 nm. Plotting was performed using the GraphPad Prism 5 software (La Jolla, CA).

EtBr Displacement Assay

An EtBr competitive binding assay was performed by recording the emission spectra of solutions containing different concentrations of ule or col (0.1–1 M) and constant concentrations of CT-DNA (0.1 M) and EtBr (0.01 M) in 0.01 M Tris–HCl buffer (pH 7.4) at room temperature. The fluorescence intensity was read at an excitation wavelength of 510 nm and an emission wavelength of 590 nm using a SpectraMax M5 Microplate Reader (Molecular Devices, US). Apparent fluorescence intensities were evaluated using the following equation: [15]

$$F\,(\%) = (I{-}I_0)/(I_{100}{-}I_0)\ \times\ 100 \qquad (1)$$

where F and I are the relative fluorescence and emission intensities for EtBr-DNA mixtures at 590 nm following the addition of borates and I_0 and I_{100} are the emission intensities of free EtBr and EtBr-CT-DNA mixtures.

DNA Cleavage and Mobility Experiments

The cleavage of calf thymus DNA (CT-DNA) and plasmid DNA was monitored using agarose gel electrophoresis. Different concentrations of borates were incubated with CT-DNA (50 ng/μl) or pUC19 plasmid DNA (11 ng/μl) at 37 °C for 1–2 h, mixed with Tris-acetate–EDTA (TAE) and run on a 0.8–1 % agarose gel containing 1 μg/ml of ethidium bromide. Gels were run at 70 V for 90 min in TAE buffer, and the bands were visualized under UV light.

Circular Dichroism Spectroscopy

A Jasco J-815 spectropolarimeter (Jasco, UK) was used to record the CD spectra of CT-DNA and borate mixtures within 200–300-nm range. A quartz cell with a path length of 0.1 cm was utilized for all measurements. Buffer subtraction was applied for all measurements by subtracting the CD spectrum of 10 mM Tris–HCl through baseline correction. Titration experiments were performed by titrating varying concentrations of borates (0.025–0.2 mM) on a constant concentration of CT-DNA (0.2 mM). Five scans of accumulation were taken for each nanometer from 300 to 200 nm with a scan speed of 50 nm/min, and the sample temperature was maintained at 25 °C.

FT-IR Spectroscopy

FT-IR spectra of borate-CT-DNA mixtures were obtained using a Nicolet 6700 FT-IR Spectrometer (Thermo Scientific,

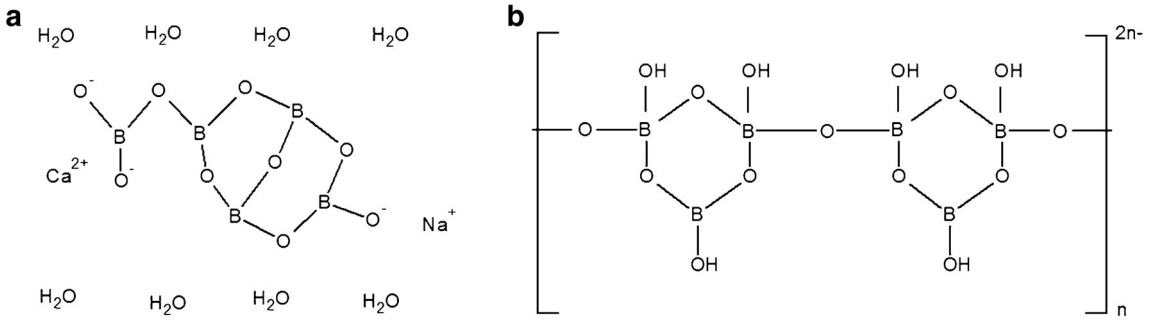

Fig. 1 Chemical structures of (**a**) ulexite and (**b**) colemanite

USA) equipped with a deuterated triglycine sulfate (DTGS) detector and a KBr beamsplitter. Spectra of borate/CT-DNA complexes were accumulated in the spectral range of 1800–600 with a 4-cm^{-1} resolution. A total of 128 scans were performed for each sample. Background spectra of blank wells were collected prior to each measurement. Varying concentrations of borates (0.1–2 mM) were incubated with a final DNA concentration of 1 mg/ml for 3 h, and 20 μl of this mixture was dried on a 96-well plate at 37 °C for 1 h prior to FT-IR transmittance analysis. All measurements were performed at room temperature and a controlled ambient humidity of 45 % RH. The absorption spectrum of Tris–HCl buffer was recorded and then subtracted from the spectra of free CT-DNA and borate/CT-DNA complexes. The spectroscopy software OMNIC™ was used for measurements, baseline corrections, buffer peak subtractions, and background corrections for H_2O and CO_2. The optical spectroscopy software Spekwin32 was used for normalization and determination of peak positions [16]. Experiments were run in at least three separate batches, and each batch contained triplicate samples. All the spectra are baseline corrected and normalized to the free CT-DNA. Four-point data smoothing was performed by Savitzky–Golay functionality prior to peak evaluation. Infrared spectra of free borates were also recorded and subtracted from the spectra of borate/CT-DNA complexes prior to analysis. In order to ensure that the observed changes in the band positions and intensities were due to the interaction of CT-DNA with borates, difference spectra [(borate/CT-DNA complexes)−(borate)] were generated after normalization.

Results and Discussion

UV–vis Absorbance Spectra

Correlations between the structure of a material and its absorbance in the UV–vis region can be used to analyze the interactions between a biomacromolecule and its ligand. It is known that hyperchromisms in DNA absorbance following the binding of a ligand may indicate the presence of a strong intercalative binding interaction (i.e., insertion between the base pairs) between that ligand and DNA [17], while hypochromisms are associated with charge-transfer interactions [18]. The reverse trend is true for the absorption spectra of the ligand: Hypochromisms and red shifts are caused by intercalative binding, while hyperchromism is associated with an electrostatic mode of interaction [19].

UV–vis absorption spectra of borate/CT-DNA complexes were analyzed to determine the mode of binding between borates and DNA. Absorbance measurements were first performed at a constant concentration of CT-DNA and varying amounts of ule or col (Fig. 2a, b). These spectra display a characteristic absorbance peak at 258 nm, which experiences slight hyperchromic shifts following the addition of borate

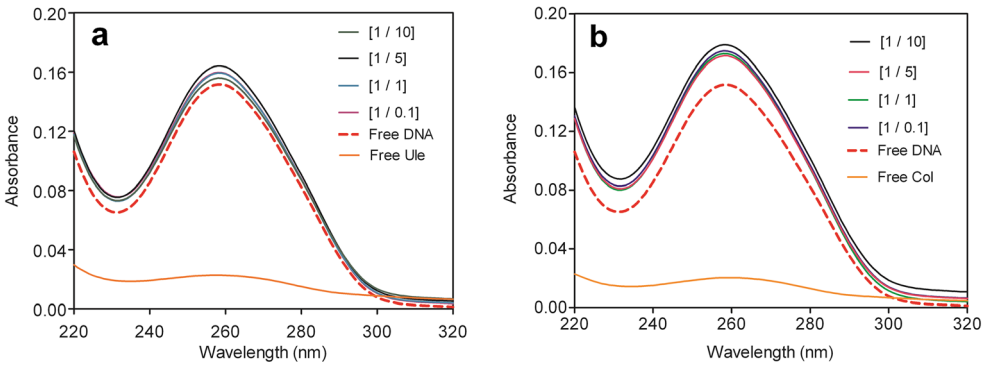

Fig. 2 UV–vis absorption spectra (220–320 nm) of CT-DNA (0.01 mM) in the presence (*solid line*) and absence (*dashed line*) of different concentrations of **a** ule and **b** col at the following ratios: [DNA/borate]=0:1, 1:0.1, 1:1, 1:5, and 1:10

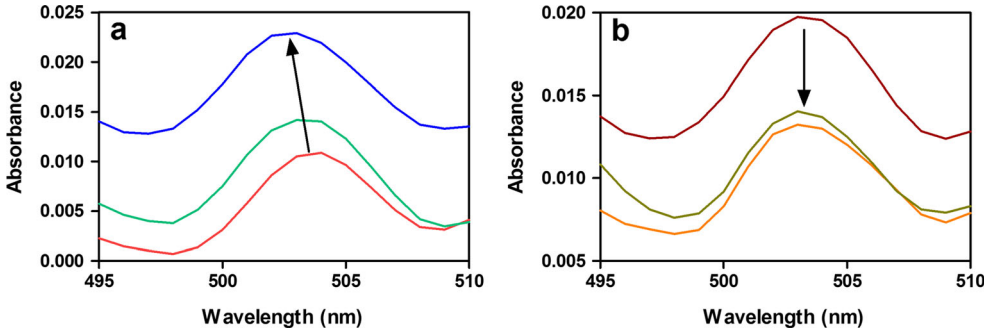

Fig. 3 UV–vis absorption spectra (495–515 nm) of **a** ule and **b** col at a constant concentration of 0.1 mM in the presence and absence of different concentrations of CT-DNA at the following ratios: [DNA/borate]= 0:1, 1:1, and 2:1

compounds, suggesting intercalative binding might be responsible for the interactions of borates with CT-DNA. This hyperchromicity is observed to be more pronounced (~20 %) for col as compared with ule (10 %). UV–vis absorbance measurements were also performed at a constant concentration of borates and varying concentrations of CT-DNA (Fig. 3a, b). UV–vis absorbance spectra of both boron compounds display a maximal absorbance peak at 503 nm. While ule samples display concentration-dependent hyperchromisms and a slight blue shift following DNA binding, col samples display a gradual hypochromism in the 503-nm band. The behavior of the ule samples is consistent with an electrostatic association between the negatively charged phosphate backbone and positively charged metal cations present in the borate structure [19, 20]. However, col samples display hypochromism rather than hyperchromism, which may indicate that col has a stronger affinity for CT-DNA and partial intercalative binding might occur for col–DNA interactions. The results in two different experiments are consistent with each other, since col samples exhibit more remarkable differences in both cases.

Competitive DNA Binding Between Ethidium Bromide and Borates

EtBr is a well-known intercalator and enjoys widespread use in anticancer research for the investigation of the intercalative capabilities of therapeutic molecules [21]. Molecules capable of intercalating with DNA strands displace EtBr moieties already present in these locations, which results in changes in the maximum absorbance of EtBr-bound DNA and yields information about the binding mode of the molecule in question [22].

EtBr displacement assay results indicate that boron compounds cannot efficiently displace EtBr from DNA (Table 1). The presence of competing DNA intercalators decreases the fluorescence of EtBr-bound DNA by about 50 %, due to the lower fluorescence intensity associated with free EtBr molecules that are displaced from their original positions by the intercalator [23]. However, the addition of borates results in slight decreases in fluorescence intensity (by 10 and 11 % for ule and col, respectively). These values are comparable to these shown by some groove binders [23], and the addition of col has resulted in more prominent decreases in the fluorescence intensity of EtBr at higher concentrations. As such, the displacement assay results suggest that ule and col use non-intercalative modes of binding to interact with DNA; however, col has a stronger affinity to CT-DNA.

DNA Cleavage and Mobility Experiments

The endonucleolytic cleavage of DNA is induced by the presence of oxygen or hydroxide radicals, which are created due to the accumulation of metal ions around the DNA helix [24]. In addition, it is known that intercalative or electrostatic binding interactions decrease the mobility of DNA in agarose gel electrophoresis [25]. Agarose gel electrophoresis results of borate-bound CT-DNA and borate-bound plasmid DNA are shown in Fig. 4. The migration of CT-DNA and plasmid DNA bands is not retarded as the borate concentration is increased, and the fragmentation of both col and ule groups is comparable with control (non-borate treated) DNA, suggesting that no DNA cleavage occurs in response to borate binding for both CT-DNA and plasmid DNA.

The observed lack of DNA cleavage activity in the presence of higher concentrations of ule and col suggests that the borates prefer a non-intercalative mode of binding and do not disrupt the structure of DNA. This result is consistent with our EtBr displacement assay results, as the borates were also unable to replace a known intercalator from the structure of DNA.

Table 1 Ethidium bromide displacement assay results showing the fluorescence intensity changes with respect to different concentrations of borates

[DNA]/[borate] molar ratio	Relative fluorescence intensity (%)	
	[DNA]/[ule]	[DNA]/[col]
1:0	100±4.1	100±4.1
1:1	96±2.7	96±3.3
1:5	95±3.9	90±1.8
1:10	90±1.6	89±2.5

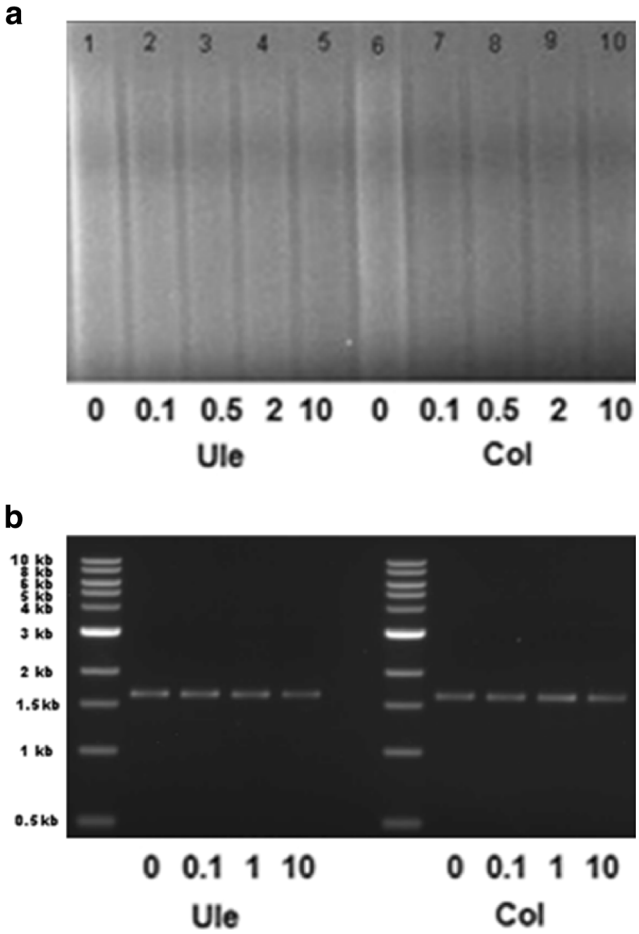

Fig. 4 Agarose gel electrophoresis bands of **a** CT-DNA (50 ng/μl) and **b** pUC19 plasmid DNA (11 ng/μl) in the presence and absence of varying concentrations of borates (0, 0.1, 0.5, 2, 10; and 0, 0.1, 1, 10 mM, respectively)

CD Spectra

The near-UV CD spectrum of B-DNA displays two positive peaks at 220 and 275 nm, and a negative peak at 245 nm [26]. It is reported that the peak at 275 nm corresponds to base stacking, and the peak at 245 nm corresponds to polynucleotide helicity of DNA [27]. In addition, a red shift at 220 nm and an intensity increase at 275-nm peaks are some of the characteristics for B to A conformational change [28]. Figure 5a, b shows CD spectra of CT-DNA in the presence of increasing concentrations of boron compounds. As shown in Fig. 5a, b, interactions with both boron compounds decrease the intensities of CD values at 245 and 275 nm, and no consistent change at 220 is observed, which may indicate that the right-handed helicity of B-DNA is modified [27] with slight changes in the base stacking interactions. Since there is no peak shift in the spectra of both samples and no increase in the intensity at 275 nm is observed, the changes in the CD spectra are not indicative for a B to A conformational transition. It is known that, while intercalators are known to increase the intensities of both positive and negative bands, groove binders show less or no perturbation on the helicity and base stacking bands of DNA [29]. For both boron compounds, there is no increase in the intensities of positive and negative peaks and the changes in the overall spectra are not so prominent, suggesting ule and col can bind to CT-DNA through non-intercalative interactions (e.g., groove binding, electrostatic interactions).

Therefore, the results of CD spectra suggest the helicity of B-DNA was modified without an alteration in the DNA's secondary structure. CT-DNA does not display major conformational changes in the presence of ule or col.

FT-IR Spectra

FT-IR spectroscopy is a nondestructive technique used in the detection of chemical bonds and the alterations in the angles and structures of these bonds following the binding of another molecule. The FT-IR spectrum of DNA features four distinct

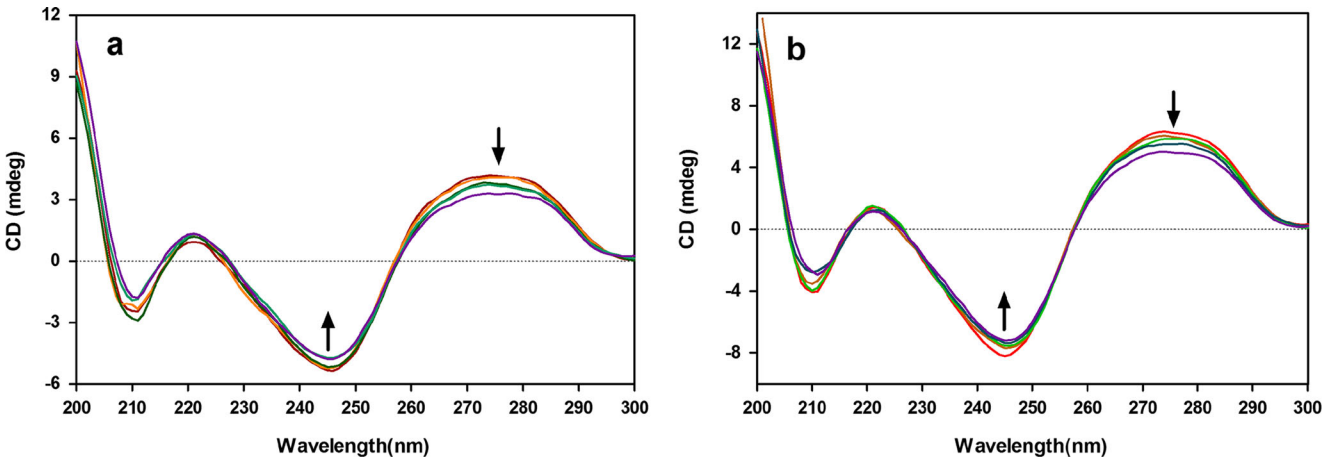

Fig. 5 CD spectra of CT-DNA (0.2 mM) in the presence of increasing amounts of **a** ule and **b** col at the following ratios: [borate/DNA]=0:1, 1:8, 1:4, 1:2, and 1:1

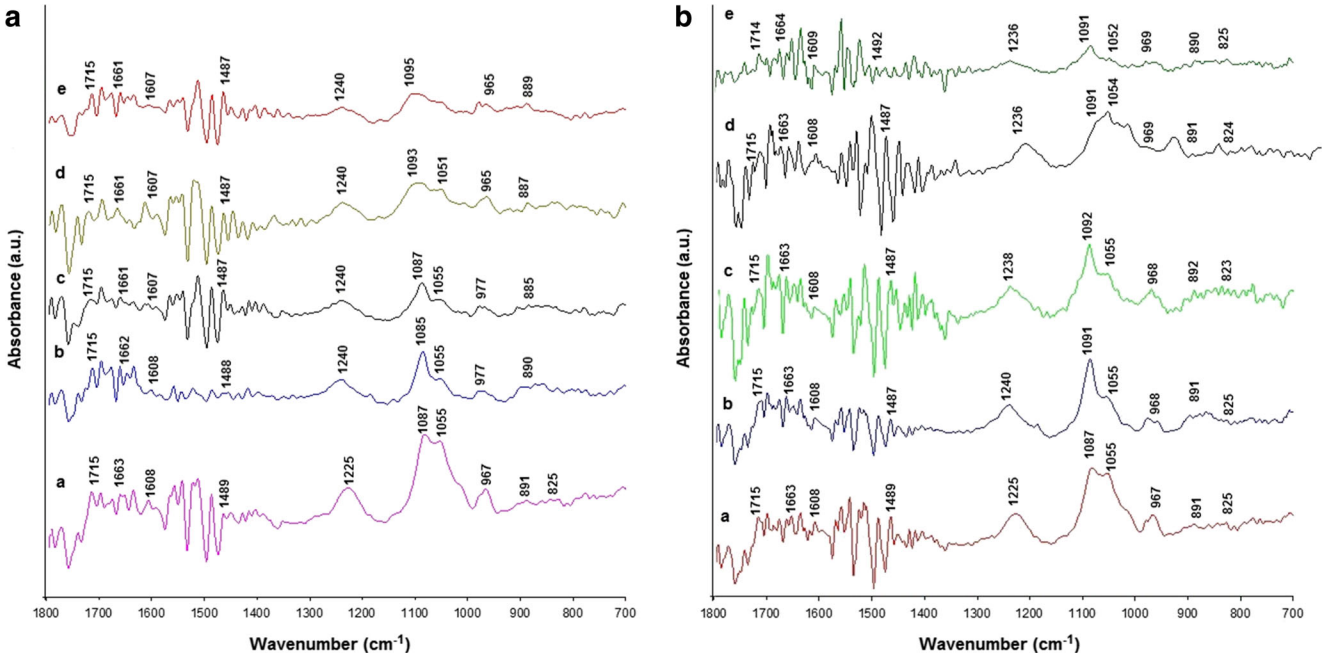

Fig. 6 FT-IR spectra of **a** CT-DNA-ule mixtures and **b** CT-DNA-col mixtures at different concentrations of borates. a–e: *a* free CT-DNA (1 mg/ml), *b* CT-DNA (1 mg/ml)+borate (0.1 mM), *c* CT-DNA (1 mg/ml)+borate (0.5 mM), *d* CT-DNA (1 mg/ml)+borate (1 mM), and *e* CT-DNA (1 mg/ml)+borate (2 mM) in the spectral region of 1800–700 cm^{-1}

peaks, which yield information about the vibrational state of DNA [28]. These are in-plane double bond vibrations of the bases, vibrations of the glycosidic linkage between a DNA base and its sugar, antisymmetric and symmetric phosphate vibrations, and phosphate-sugar backbone vibrations which are observed in the region of 1800–700 cm^{-1} [30]. Specific marker bands can be used to characterize the conformation of DNA, which may change between A, B, and Z geometries depending on environmental conditions or binding of a molecule [30].

Figure 6 shows the infrared spectrum of the free DNA and its complexes with ule and col. All peak assignments of DNA were made in accordance with the literature [31]. The band at 1715 cm^{-1} reflects the in-plane vibrations of guanine stretching, while the band at 1663 cm^{-1} is attributed to thymine stretching vibrations. The bands at 1604 and 1489 cm^{-1} are associated with the ring stretching vibrations of adenine and cytosine, respectively [32]. No major shifts were observed in peaks associated with DNA bases for borate concentrations of up to 2 mM, but the cytosine-associated band at 1487 cm^{-1}

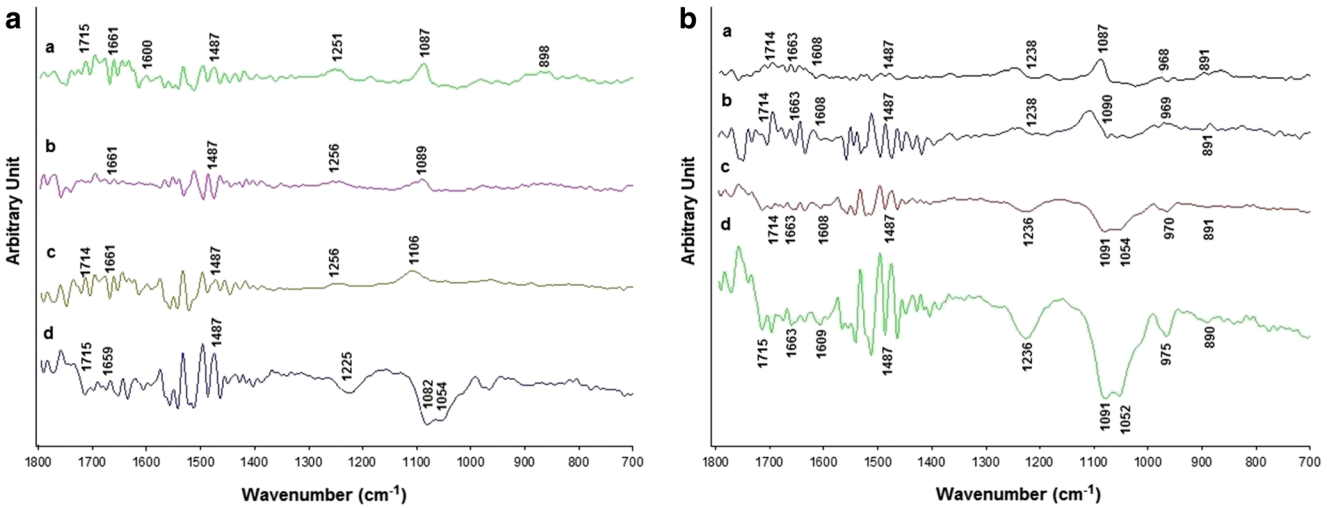

Fig. 7 FT-IR difference spectra of **a** CT-DNA-ule mixtures and **b** CT-DNA-col mixtures within the spectral region of 1800–700 cm^{-1}. a–d: *a* CT-DNA (1 mg/ml)+borate (0.1 mM), *b* CT-DNA (1 mg/ml)+borate (0.5 mM), *c* CT-DNA (1 mg/ml)+borate (1 mM), and *d* CT-DNA (1 mg/ml)+borate (2 mM)

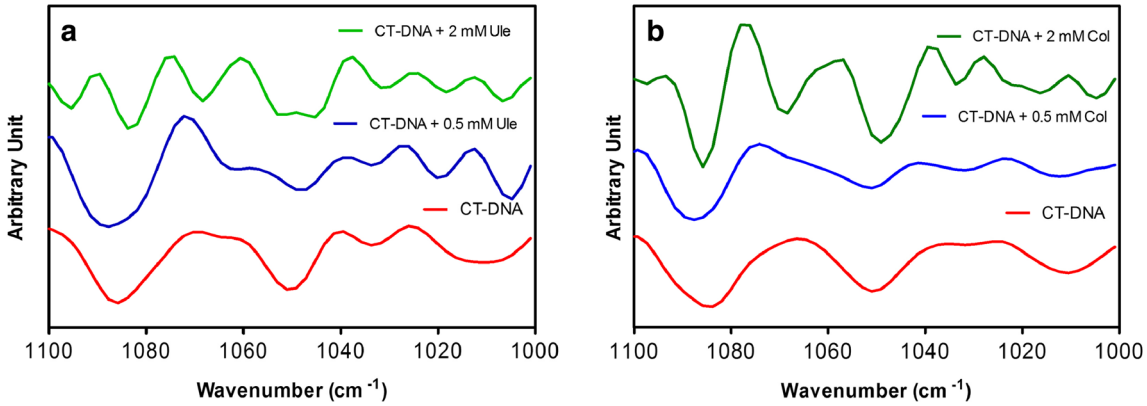

Fig. 8 FT-IR second-derivative spectra of **a** CT-DNA-ule mixtures and **b** CT-DNA-col mixtures within the spectral region of 1100–1000 cm^{-1}

was enhanced in a concentration-dependent manner in the difference spectra of borate/CT-DNA complexes. Higher concentrations of ule and col were observed to slightly disrupt base vibrations, resulting in 1–2 cm^{-1} shifts. The peak at 1225 cm^{-1} is attributed to phosphate asymmetric stretching and shows an upward shift to 1240 cm^{-1} following the binding of ule and col to CT-DNA. The phosphate symmetric stretching peak, located at 1087 cm^{-1}, also shifts to 1095 cm^{-1} following ule binding. Similarly, the presence of col causes major shifts at these bands (11–13 cm^{-1}). The difference spectra of borate-bound CT-DNA also display large shifts in the locations and intensities of 1225- and 1087-cm^{-1} peaks, which are associated with asymmetric and symmetric phosphate peaks (Fig. 7). Furthermore, the second-derivative analysis of the FT-IR spectra indicates several significant peak shifts and intensity changes of the symmetric phosphate peaks of borate/CT-DNA complexes, especially at higher concentrations of both ule and col (Fig. 8). These changes may result from electrostatic interactions of positively charged ions in the structures of the borates and the negatively charged phosphate groups of DNA. Infrared bands at 1055 cm^{-1} reflect deoxyribose sugar vibrations, associated with C=O and C-C stretching within the sugar structure, while sugar-phosphate vibrations are present at 967 cm^{-1} in the spectrum of free CT-DNA. Figure 8 indicates that the intensity of these bands decrease significantly following the addition of ule and col, especially at higher concentration of borates. The DNA backbone band at 967 cm^{-1} shifts to 965–977 cm^{-1} in the presence of ule and shows 1–2 cm^{-1} upward shifts following the addition of col. The binding of borate compounds to the phosphate groups also alters the bands associated with the phosphate backbone, which can be seen in the difference spectra of borate/CT-DNA complexes. Minor shifts are also observed in the deoxyribose sugar vibrations (~3 cm^{-1}) of borate-bound CT-DNA. The peak at 825 cm^{-1} is a B-DNA conformation marker and appears at 825 cm^{-1} for different concentrations of ule–DNA complexes, but shifts to 823–824 cm^{-1} following complex formation with col.

The change in the locations and intensities of $–PO_2$ bands is a strong indicator of the interaction of DNA backbone phosphates with borates. Our results suggest that borates bind externally to the sugar-phosphate backbone of the CT-DNA double helix. In addition, the general lack of base-related peak shifts is in line with our CD results and suggests that a non-intercalative binding mode is utilized by boron compounds for DNA binding.

Conclusions

We have investigated and compared the interactions of two common natural borates with CT-DNA. Our results indicate that both boron compounds can bind to CT-DNA with sharing similar DNA binding characteristics. Boron compounds do not appear to cause the unwinding of the DNA helix or any other significant change in its secondary structure. Furthermore, our spectroscopy analysis results suggest that both compounds interact with DNA under a non-intercalative mode of binding, which is consistent with the reported lack of toxicity for these materials [9]. FT-IR spectra of both ule and col reveal that the borates might interact with DNA through sugar-phosphate backbone binding. Overall, we describe the binding patterns of two borate compounds to CT-DNA and provide further insight into understanding the biological importance of these borates.

Acknowledgments The authors are thankful to the Turkish National Boron Research Institute (Ulusal Bor Araştırma Enstitüsü (BOREN), Ankara, Turkey) for financial support through Research Grant No. 2012.ç0356 and to E. Kalyoncu, A. D. Özkan, and R. T. Gursacli for their help and support in conducting the experiments described. A. Ozdemir is supported by TUBITAK BIDEB (2211) PhD fellowship. O.F. Sarioglu acknowledges TUBITAK BIDEB (2211-C) for National PhD Scholarship.

References

1. Davis SM, Drake KD, Maier KJ (2002) Toxicity of boron to the duckweed, Spirodella polyrrhiza. Chemosphere 48:615–620
2. Loomis WD, Durst RW (1992) Chemistry and biology of boron. Biofactors 3:229–239
3. Pandey N, Gupta B (2013) The impact of foliar boron sprays on reproductive biology and seed quality of black gram. J Trace Elem Med Biol 27:58–64
4. Nielsen FH (1994) Biochemical and physiologic consequences of boron deprivation in humans. Environ Health Perspect 102(Suppl 7):59–63
5. Nielsen FH, Hunt CD, Mullen LM, Hunt JR (1987) Effect of dietary boron on mineral, estrogen, and testosterone metabolism in postmenopausal women. FASEB J 1:394–397
6. Ince S, Kucukkurt I, Cigerci IH, Fatih Fidan A, Eryavuz A (2010) The effects of dietary boric acid and borax supplementation on lipid peroxidation, antioxidant activity, and DNA damage in rats. J Trace Elem Med Biol 24:161–164
7. Turkez H (2008) Effects of boric acid and borax on titanium dioxide genotoxicity. J Appl Toxicol 28:658–664
8. Turkez H, Tatar A, Hacimuftuoglu A, Ozdemir E (2010) Boric acid as a protector against paclitaxel genotoxicity. Acta Biochim Pol 57: 95–97
9. Türkez H, Geyikoğlu F, Tatar A, Keleş S, Ozkan A (2007) Effects of some boron compounds on peripheral human blood. Z Naturforsch C 62:889–896
10. Rodríguez-Pulido A, Aicart E, Llorca O, Junquera E (2008) Compaction process of calf thymus DNA by mixed cationic-zwitterionic liposomes: a physicochemical study. J Phys Chem B 112:2187–2197
11. Ramakrishnan S, Suresh E, Riyasdeen A, Akbarsha MA, Palaniandavar M (2011) DNA binding, prominent DNA cleavage and efficient anticancer activities of tris(diimine)iron(II) complexes. Dalton Trans 40:3524–3536
12. Cetin B, Unal HI, Erol O (2012) The negative and positive electrorheological behavior and vibration damping characteristics of colemanite and polyindene/colemanite conducting composite. Smart Mater Struct 21:125011
13. Ulexite (n.d.) ChemicalBook Inc.http://www.chemicalbook.com/ProductChemicalPropertiesCB71074735_EN.htm. Accessed 04 May 2015
14. Chen LM, Liu J, Chen JC, Tan CP, Shi S, Zheng KC, Ji LN (2008) Synthesis, characterization, DNA-binding and spectral properties of complexes [Ru(L)4(dppz)]2+ (L=Im and MeIm). J Inorg Biochem 102:330–341
15. Strand SP, Danielsen S, Christensen BE, Vårum KM (2005) Influence of chitosan structure on the formation and stability of DNA-chitosan polyelectrolyte complexes. Biomacromolecules 6: 3357–3366
16. F. Menges "Spekwin32 - optical spectroscopy software", Version 1.71.6.1, 2013, http://www.effemm2.de/spekwin/
17. Wu SS, Yuan WB, Wang HY, Zhang Q, Liu M, Yu KB (2008) Synthesis, crystal structure and interaction with DNA and HSA of (N, N'-dibenzylethane-1,2-diamine) transition metal complexes. J Inorg Biochem 102:2026–2034
18. Markovitsi D (2009) Interaction of UV radiation with DNA helices. Pure Appl Chem 81:1635–1644
19. Sirajuddin M, Ali S, Badshah A (2013) Drug-DNA interactions and their study by UV-Visible, fluorescence spectroscopies and cyclic voltametry. J Photochem Photobiol B 124:1–19
20. Eshkourfu R, Čobeljić B, Vujčić M, Turel I, Pevec A, Sepčić K, Zec M, Radulović S, Srdić-Radić T, Mitić D, Andjelković K, Sladić D (2011) Synthesis, characterization, cytotoxic activity and DNA binding properties of the novel dinuclear cobalt(III) complex with the condensation product of 2-acetylpyridine and malonic acid dihydrazide. J Inorg Biochem 105:1196–1203
21. Ting CY, Hsu CT, Hsu HT, Su JS, Chen TY, Tarn WY, Kuo YH, Whang-Peng J, Liu LF, Hwang J (2013) Isodiospyrin as a novel human DNA topoisomerase I inhibitor. Biochem Pharmacol 66: 1981–1991
22. Ju CC, Zhang AG, Yuan CL, Zhao XL, Wang KZ (2011) The interesting DNA-binding properties of three novel dinuclear Ru(II) complexes with varied lengths of flexible bridges. J Inorg Biochem 105:435–443
23. Kelly JM, Tossi AB, McConnell DJ, OhUigin C (1985) A study of the interactions of some polypyridylruthenium (II) complexes with DNA using fluorescence spectroscopy, topoisomerisation and thermal denaturation. Nucleic Acids Res 13:6017–6034
24. Stohs SJ, Bagchi D (1995) Oxidative mechanisms in the toxicity of metal ions. Free Radic Biol Med 18:321–336
25. Kumar RS, Arunachalam S (2009) DNA binding and antimicrobial studies of polymer-copper(II) complexes containing 1,10-phenanthroline and L-phenylalanine ligands. Eur J Med Chem 44: 1878–1883
26. Ivanov VF, Minchenkova LE, Schyolkina AK, Poletayer AI (1973) Different conformations of double-stranded nucleic acid in solution as revealed by circular dichroism. Biopolymers 12:89–110
27. Kunwar A, Simon E, Singh U, Chittela RK, Sharma D, Sandur SK, Priyadarsini IK (2011) Interaction of a curcumin analogue dimethoxycurcumin with DNA. Chem Biol Drug Des 77:281–287
28. Jangir DK, Charak S, Mehrotra R, Kundu S (2011) FTIR and circular dichroism spectroscopic study of interaction of 5-fluorouracil with DNA. J Photochem Photobiol B 105:143–148
29. Uma V, Elango M, Nair BU (2007) Copper(II) terpyridine complexes: effect of substituent on DNA binding and nuclease activity. Eur J Inorg Chem 22:3484–3490
30. Mantsch HH, Chapman D (1996) Infrared spectroscopy of biomolecules. A John Wiley & Sons, Inc., New York
31. Adali T, Bentaleb A, Elmarzugi N, Hamza AM (2013) PEG-calf thymus DNA interactions: conformational, morphological and spectroscopic thermal studies. Int J Biol Macromol 61:373–378
32. Agarwal S, Jangir DK, Singh P, Mehrotra R (2014) Spectroscopic analysis of the interaction of lomustine with calf thymus DNA. J Photochem Photobiol B 130:281–286